

Fermi-level pinning at nickel disilicide–silicon interface

Akira Kikuchi

Central Research Laboratory, Hitachi, Ltd., Kokubunji, Tokyo 185, Japan

(Received 4 January 1989)

It has been found that the single-crystal NiSi₂ Schottky-barrier height changes from 0.65 to 0.79 eV, depending upon the type-*B* NiSi₂ film thickness on Si(111). In this study, the barrier height is calculated by an interface-defect model and compared with our experimental results. The calculated barrier height seems to give a good explanation of our experimental results.

I. INTRODUCTION

Recently published results^{1–4} of single-crystal silicide-Si interfaces have generated great interest since these interfaces are of basic importance to the understanding of Schottky-barrier formation. Silicon is devoid of many of the interfacial complexities of compound semiconductors. Its surface can be cleaned thoroughly in an ultrahigh vacuum (UHV). Therefore, single-crystal silicide-Si interfaces with a high degree of structural perfection can be obtained. In particular, since the lattice mismatch between NiSi₂(111) and Si(111) is only 0.45%, NiSi₂ can be grown epitaxially on a Si(111) substrate, offering a simple interfacial heterostructure.

Tung^{1,5} has revealed that high Schottky-barrier height (0.78–0.79 eV) can be obtained by carefully controlling silicide-formation conditions, and he also reported Schottky-barrier heights of 0.65 eV for type-*A* NiSi₂ and 0.79 eV for type-*B* NiSi₂. These types correspond to nontwinned and twinned structures, respectively. The orientation of type-*A* NiSi₂ is identical to that of the Si(111) substrate. The orientation of type-*B* NiSi₂ is rotated 180° about the surface-normal direction with respect to the Si substrate. On the other hand, Liehr *et al.*² suggest that high barrier height (0.78 eV) is obtained only for near-perfect interfaces. Less-perfect interfaces yield low barrier height (0.66 eV). Their results suggest that the variation of barrier height depends primarily on the structural perfection of the Ni silicide–Si interface, and that the type of NiSi₂ is not important. Recently, we indicated that the barrier height changed from 0.65 to 0.79 eV dependent upon the type-*B* NiSi₂ film thickness (perhaps the degree of perfection of the NiSi₂/Si interface).⁶

In this study, the theoretical calculations were made using an interface-defect model⁷ to explain our experimental results.

II. RESULTS AND DISCUSSION

Models for explaining Schottky-barrier height can be categorized into two broad groups:⁸ linear and nonlinear models. For the linear model, the barrier height depends on the bulk parameters of the metal and semiconductor. The barrier height changes linearly for small variations of these parameters. For the nonlinear model, however, the

barrier height is not sensitive to the bulk parameters. The interfacial electronic structures, such as electrically active impurities and defects, play a significant role.

A. Fermi-level pinning by interface-defect model

Figure 1 shows our measured Schottky-barrier height^{6,9–12} as a function of Miedema's electronegativity,¹³ which is given by $(X_M^m X_{Si}^n)^{1/(m+n)}$ for silicides $M_m Si_n$. The Schottky-barrier diodes were prepared on *n*-type, $\langle 100 \rangle$ - and $\langle 111 \rangle$ -oriented Si wafers (5 Ω cm) using the same procedures. The detailed cross section of a Schottky-barrier diode and the process technology have been reported in our previous papers. The experimental data in Fig. 1 are obviously categorized into two groups. The barrier height indicated by the solid line is determined by the metal-induced gap states (MIGS) model.^{14,15} On the other hand, the barrier height indicated by the dashed line is determined by an interface-defect model.^{7,16,17} As stated before, the Schottky-barrier height of type-*B* NiSi₂ changes from 0.65 to 0.79 eV, dependent upon the NiSi₂ film thickness. Low barrier height (0.65 eV) is obtained for a thick type-*B* NiSi₂ film (≥ 50 nm)

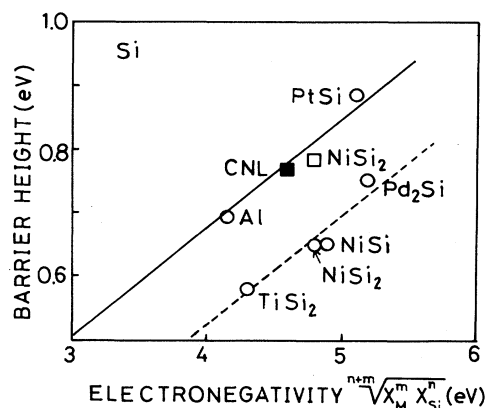


FIG. 1. Measured Schottky-barrier height as a function of Miedema's electronegativity. For silicide $M_m Si_n$, the geometric mean of the metal and Si electronegativities is taken. CNL represents the charge-neutrality level calculated by Tersoff (Ref. 15).

TABLE I. Sample-preparation parameters and Schottky-barrier height.

Metal	Deposition	Silicide formation (°C)	Vacuum (Pa)	Barrier height (eV)
Al	Al (EB ^a)		10 ⁻⁵	0.69
PtSi	Pt (EB)	440	10 ⁻⁵	0.85
Pd ₂ Si	Pd (EB)	250	10 ⁻⁵	0.75
TiSi ₂	Ti (EB)	600	10 ⁻⁵	0.58
NiSi	Ni (MBE ^b)	400	10 ⁻⁸	0.65
NiSi ₂	Ni+Si (MBE)	400	10 ⁻⁸	0.65–0.79

^aElectron-beam (EB) evaporation (ULVAC, EBS10A).

^bMolecular-beam epitaxy (MBE) (VG Semicon., V80).

and high barrier height (0.79 eV) for a thin type-B NiSi₂ (~1 nm). Figure 1 suggests that high barrier height is determined by the MIGS model, whereas low barrier height is determined by the interface-defect model.

Sample-preparation parameters and Schottky-barrier height are summarized in Table I. Nickel disilicide (NiSi₂) was formed on Si(100) and Si(111) substrates by the codeposition of Ni and Si at 400 °C in UHV. Other silicides were formed by the reaction of metals deposited at low temperature with Si(100) substrates.

An energy-band diagram of NiSi₂/Si contact under thermal equilibrium is shown in Fig. 2. The interface donor-defect level, which is located at 0.62 eV from the conduction-band edge at the interface, is chosen to agree with the value for Si.⁸ The dashed line indicates the interface-defect distribution. The calculations in this study, however, assume that these donors are all located at the level of 0.62 eV in the band gap. In addition, the interface states have only two charge states: neutral or charged.

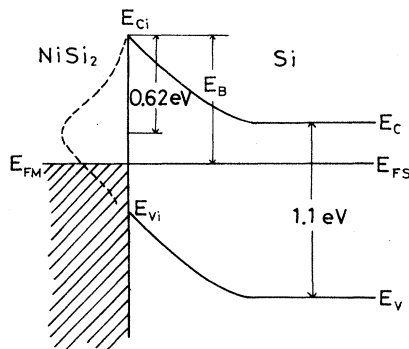


FIG. 2. Energy-band diagram of NiSi₂/Si(111) contact under thermal equilibrium. E_C and E_V are conduction- and valence-band energies. E_{Ci} and E_{Vi} indicate those at the interface. E_B ($q\phi_B$) is Schottky-barrier height. E_{FM} and E_{FS} are the Fermi level of NiSi₂ and Si, respectively. The interface-defect level is located at 0.62 eV under the conduction-band edge at the interface.

The schematic metal-semiconductor interface given by Zur⁷ is shown in Fig. 3. The Fermi-level position when all the defects are located in a single plane at $x=d$ is given by⁷

$$q(\phi_m + \Delta V_m - \chi) = -\eta(d) + \frac{q^2 d}{\epsilon \epsilon_0} [N_D^+(\eta(d))] \quad (1)$$

and

$$N_D^+(\eta) = \frac{N_D}{2 \exp\left[\frac{\eta + E_c - E_s}{kT}\right] + 1}, \quad (2)$$

where ϕ_m is the metal work function, χ is the semiconductor electron affinity, ΔV_m is the potential difference between the jellium surface and the bulk, $\eta(d)$ is the Fermi-level position from the conduction-band edge at the interface, q is the electron charge (positive), ϵ is the dielectric constant of the semiconductor, ϵ_0 is the free-space permittivity, N_D is the defect density in the band gap, and N_D^+ is the (positively) ionized defect density. In the following, the interfacial width, d , was taken to be 0.5 nm. Since the Fermi-level position is mainly determined by the interface charge contribution,⁷ the bulk contribu-

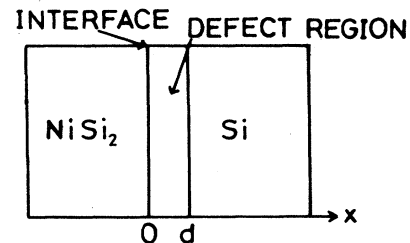


FIG. 3. Schematic drawing of the metal-semiconductor interface. The metal-semiconductor system consists of three regions: semi-infinite bulk metal, semi-infinite bulk semiconductor, and defect region. All the defects are localized in the region $0 \leq x \leq d$, and in this study, they are all on $x=d$. The calculations are made on the plane $x=d$.

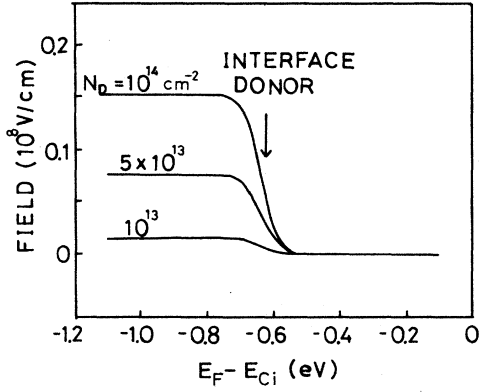


FIG. 4. Electric field vs Fermi-level position in the gap at $x=0.5$ nm, for defect densities of 10^{13} – 10^{14} cm^{-2} .

tion term is neglected in Eq. (1).

Figure 4 shows the electric field in the interface layer as a function of η ($=E_F - E_{Ci}$), the relative Fermi-level position, for three different values of defect density. As stated previously, the interface-defect level is chosen to agree with the value for Si-defect donor. It can be seen that the defect contribution to the electric field becomes large with an increase in defect density.

The Fermi-level position with respect to the valence-band edge at the interface is shown in Fig. 5 as a function of $\phi_m + \Delta V_m^0 - \chi$ for four different values of defect density. ΔV_m was calculated from⁷

$$\begin{aligned} \Delta V_m(\Delta Q_m) &= \Delta V_m^0 + \left[\frac{\partial \Delta V_m}{\partial Q_m} \right]_0 \Delta Q_m \\ &= \Delta V_m^0 + \left[\frac{0.1 \text{ V}}{10^{14} \text{ cm}^{-2}} \right] \Delta Q_m. \end{aligned} \quad (3)$$

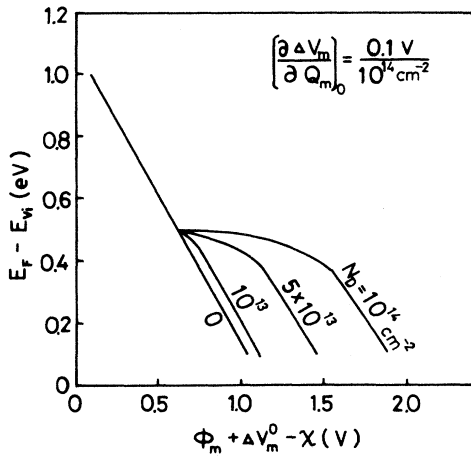


FIG. 5. Fermi-level position as a function of $\phi_m + \Delta V_m^0 - \chi$ for four defect densities.

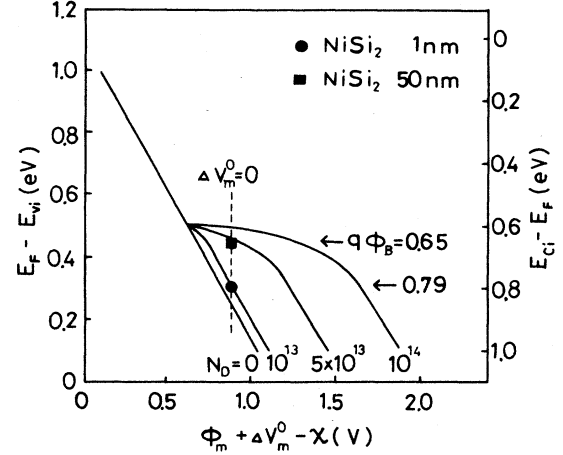


FIG. 6. Comparison of measured NiSi_2 Schottky-barrier height with those calculated using the interface defect model.

It is clearly seen that the Fermi level is pinned at the defect level (0.48 eV), until the defects are all charged, and moves towards the valence-band edge at the interface in parallel with the line corresponding to the MIGS model ($N_D=0$). The degree of Fermi-level pinning depends on the interface-defect density.

B. Comparison with our experiments

It has been found recently that the Schottky-barrier height can be changed by carefully controlling the type-B NiSi_2 film thickness on Si(111) substrate.⁶ Figure 6 shows the measured barrier height for two different Schottky-barrier diodes and those calculated by the interface-defect model. The work function for NiSi_2 , 4.94 eV, was obtained by taking the geometric mean of Ni (5.15 eV) and Si (4.85 eV) work functions.¹⁸ The experimental data for NiSi_2 are plotted for $\Delta V_m^0=0$. Figure 6 indicates that the high barrier height (0.79 eV) is obtained for a defect density of $1 \times 10^{13} \text{ cm}^{-2}$ and the low barrier height (0.65 eV) for a defect density of $5 \times 10^{13} \text{ cm}^{-2}$. The defect density corresponding to both barrier heights, of course, changes according to the variation of ΔV_m^0 shown in Fig. 6.

III. CONCLUSIONS

The Schottky-barrier height for the type-B $\text{NiSi}_2/\text{Si}(111)$ interface was calculated using the interface-defect model and compared with our experimental data. The reduction of barrier height could be explained by Fermi-level pinning resulting from an increase in defect density at the NiSi_2/Si interface.

ACKNOWLEDGMENTS

The author is grateful to Dr. Y. Shiraki and T. Ohshima for their helpful discussions.

- ¹R. T. Tung, *Phys. Rev. Lett.* **52**, 461 (1984).
²M. Liehr, P. E. Schmid, F. K. LeGoues, and P. S. Ho, *Phys. Rev. Lett.* **54**, 2139 (1985).
³R. J. Hauenstein, T. E. Schlesinger, T. C. McGill, B. D. Hunt, and L. J. Schowalter, *Appl. Phys. Lett.* **47**, 853 (1985).
⁴M. Ospelt, J. Henz, L. Flepp, and H. von Känel, *Appl. Phys. Lett.* **52**, 227 (1988).
⁵R. T. Tung, K. K. Ng, J. M. Gibson, and A. F. J. Levi, *Phys. Rev. B* **33**, 7077 (1986).
⁶A. Kikuchi, T. Ohshima, and Y. Shiraki, *J. Appl. Phys.* **64**, 4614 (1988).
⁷A. Zur, T. C. McGill, and D. L. Smith, *Phys. Rev. B* **28**, 2060 (1983).
⁸P. E. Schmid, *Helv. Phys. Acta* **58**, 371 (1985).
⁹A. Kikuchi, H. Yamamoto, S. Iwata, T. Ikeda, and K. Nakata, *J. Appl. Phys.* **51**, 4913 (1980).
¹⁰A. Kikuchi and S. Sugaki, *J. Appl. Phys.* **53**, 3690 (1982).
¹¹A. Kikuchi, *J. Appl. Phys.* **54**, 3998 (1983).
¹²A. Kikuchi, *Jpn. J. Appl. Phys.* **25**, L894 (1986).
¹³A. R. Miedema, P. F. el Châtel, and F. R. de Boer, *Physica B+C* **100B**, 1 (1980).
¹⁴V. Heine, *Phys. Rev.* **138**, A1689 (1965).
¹⁵J. Tersoff, *Phys. Rev. Lett.* **52**, 465 (1984).
¹⁶W. E. Spicer, P. W. Chye, P. R. Skeath, C. Y. Su, and I. Lindau, *J. Vac. Sci. Technol.* **16**, 1422 (1979).
¹⁷W. Mönch, *Phys. Rev. Lett.* **58**, 1260 (1987).
¹⁸J. L. Freeouf, *Solid State Commun.* **33**, 1059 (1980).